

## Controlled Plasticity Burnishing to Improve the Performance of Friction Stir Processed Ni-Al Bronze

Paul S. Prevey<sup>1,a</sup>, Douglas J. Hornbach<sup>2,b</sup>, Dr. N. Jayaraman<sup>3,c</sup>

<sup>1,2,3</sup>Lambda Technologies, 5521 Fair Lane, Cincinnati, OH 452296, USA

<sup>a</sup>pprevey@lambdatechs.com, <sup>b</sup>dhornbach@lambdatechs.com, <sup>c</sup>njayaraman@lambdatechs.com

### ABSTRACT

Friction stir welding (FSW) allows the joining of aluminum alloys in ways previously unattainable offering new manufacturing technology. Friction stir processing (FSP) of cast alloys such as Ni-Al bronze eliminates casting voids and improves the properties to that of wrought material. However, the local heating produced by both FSW and FSP can leave a fusion zone with reduced mechanical properties and a heat-affected zone with tensile residual stresses that can be deleterious to fatigue performance. Controlled plasticity burnishing (CPB) is an established surface treatment technology that has been investigated and described extensively for the improvement of damage tolerance, corrosion fatigue, and stress corrosion cracking performance in a variety of alloys. Mechanical CPB processing in conventional CNC machine tools or with robotic tool positioning is readily adapted to industrial FSW and FSP fabrication of components, either simultaneously or as a post process.

CPB was applied to FSP Ni-Al Bronze to produce a depth of compression of 2.5 mm and a maximum subsurface magnitude of -150 ksi. The effect of FSP on the fatigue performance in a saltwater marine environment and in the presence of foreign object damage (FOD) was documented with and without CPB processing. FSP was found to increase the fatigue strength of the Ni-Al Bronze by 70% without affecting the corrosion behavior of neutral salt solution. FSW actually produced a more noble material in the acidic salt solution. CPB after FSP mitigated damage 1 mm deep.

**Keywords:** Friction stir welding, FSW, Friction stir processing, FSP, Controlled plasticity burnishing (CPB), nickel, aluminum, bronze, Ni-Al Bronze, high cycle fatigue, (HCF), foreign object damage (FOD)

### INTRODUCTION

Friction stir processing (FSP) has been proposed as a means of developing a forged structure, with the inherent benefits of fine grain size in the hot worked stirred material, from a coarse cast structure. Nickel-aluminum bronze (NAB) castings are currently

used for marine applications, including ship propellers, where they are subject to the potential for saltwater corrosion or corrosion fatigue and foreign object damage (FOD). Casting porosity provides fatigue nucleation sites that can be eliminated, as the overall properties are improved, by FSP.

FSW, a process very similar to FSP, has been shown to introduce tensile residual stresses in aluminum alloys that can reduce fatigue performance.[1] Low plasticity burnishing (LPB) has been previously reported to restore and even improve the fatigue performance beyond that of the base metal [1] by introducing deep residual compressive stresses.

The purpose of this investigation was to document the effect of the deep compressive layer generated by controlled plasticity burnishing (CPB) on the high cycle fatigue (HCF) performance and FOD tolerance of friction stir processed NAB in a simulated marine salt water environment. The HCF performance of the FSP + CPB condition were compared to as-FSP and as-cast (baseline) conditions. The effect of FSP and CPB processing on the corrosion behavior of NAB in neutral and acidic saltwater simulated marine environments was also investigated.

### TECHNIQUE

**Material.** Four cast Ni-Al bronze plates were FSP and supplied by Rockwell Scientific. The plates were nominally 12 x 15 x 1 in. A tensile test was performed to establish the properties of the as-received NAB material, prior to FSP, is shown in the table below.

Condition	0.2 % offset Yield Strength (ksi)	Tensile Strength (ksi)	Elong. (%)
As-Cast	35.4	75.4	15.6
FSP	~60		

The nominal chemistry for the Ni-Al Bronze is shown below.

Chemistry for Ni-Al Bronze (weight percent)					
Cu	Ni	Al	Fe	Mn	Trace
81	5	9	4	1.0	Si, Sn, Zn, Co, Pb

**CPB Processing.** The basic LPB process has been described previously.[2,3,4,5] The CPB process differs only in that a controlled level of higher cold work is achieved to deliberately increase the yield and tensile strength of the material. CPB was developed for the FSP plates empirically by running trials to achieve the desired depth and magnitude of compression and cold work. CNC control code was modified to allow positioning of the CPB tool in a series of passes on the FSP side of the plate and to control the burnishing pressure to develop the desired magnitude of compressive stress. Processing was performed in a 4-axis CNC mill.

**Surface Roughness.** The Baseline material surface roughness ranged from 8.0 to 12.9  $\mu\text{in.}$  (rms). The FSP surface roughness ranged from 19.7 to 23.2  $\mu\text{in.}$ , as compared to 2.3 to 3.3  $\mu\text{in.}$  for the CPB surfaces.

**Residual Stress Measurement.** TX-ray diffraction residual stress measurements were made employing a  $\sin^2\psi$  technique and the diffraction of manganese  $K\alpha_1$  radiation from the (311) planes, of the NAB. It was first verified that the lattice spacing was a linear function of  $\sin^2\psi$ , as required for the plane stress linear elastic residual stress model. [6,7,8,9] Material was removed electrolytically for subsurface measurement. The residual stress measurements were corrected for both the penetration of the radiation into the subsurface stress gradient [10] and for stress relaxation caused by layer removal.[11] The value of the x-ray elastic constants required to calculate the macroscopic residual stress from the strain normal to the (311) planes of NAB were determined in accordance with ASTM E1426-91.[12] Systematic errors were monitored per ASTM specification E915.

The subsurface residual stress distributions produced by FSP, FSP+flash removal milling, and FSP+CPB by x-ray diffraction measurement in the directions parallel and perpendicular to the FSP tool path as shown schematically in Figure 1.

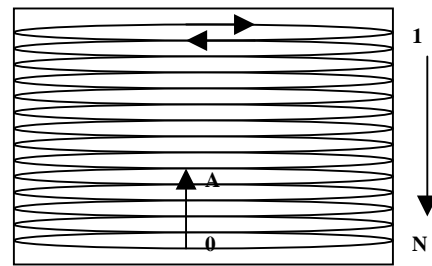


Fig. 1 – Schematic showing FSP tool path alternating from 1<sup>st</sup> to Nth pass. XRD stress measurement locations in Figs. 2 and 3, were referenced from an origin at last pass along line 0A.

### HIGH CYCLE FATIGUE TESTING

Fatigue testing was performed at ambient temperature in 4-point bending under constant amplitude loading on a Sonntag SF-1U fatigue machine at 30 Hz and a stress ratio  $R=0.1$ . The trapezoidal cross section fatigue sample used has been described previously[1]. A total of six S-N curves were generated from the following groups of specimens:

Group No.	Group Identification
1	Baseline
2	Baseline+Salt
3	FSP+Salt
4	FSP+FOD+Salt
5	FSP+CPB+Salt
6	FSP+CPB+FOD+Salt

The HCF life of susceptible alloys can be significantly reduced if the exposed surface is subjected to a corrosive environment during fatigue cycling. The test groups identified as such were tested in a potentially corrosive salt solution environment to determine if the NAB alloy was susceptible to corrosion fatigue in a salt environment after FSP and/or CPB processing. A neutral 3.5 wt% NaCl solution was used to simulate sea water, and applied to the surface of the samples at the initiation of fatigue testing.[1]

FOD can have a degrading effect on the HCF strength. FOD was simulated by 0.040 in. deep triangular electro-discharge machined (EDM) notches. EDM leaves a pre-cracked recast layer in residual tension at the bottom of the notch that has been shown to be both reproducible and more damaging than machined notches.

## ELECTROCHEMICAL POLARIZATION

Electrochemical polarization curves were obtained to determine the effect of FSP and CPB on the general corrosion properties of NAB in a marine environment. Two solutions were used: a neutral 3.5% NaCl solution with a pH of 6.25, and an acidic 3.5% NaCl solution with a pH of 3.5. The pH of the salt solution was adjusted using 2% NaOH or 1 N HCl. Three replicates tests were run for the as-cast (600 grit finish), FSP (600 grit finish), and CPB conditions. The samples were exposed to the solution in the corrosion cell for one hour prior to the start of the test to stabilize the open circuit potential (OCP). The exposure period of one hour was selected based on similar studies of NAB by Al-Hashem et al [13].

An Avesta corrosion cell [14], which enables the testing of the surface of a specimen while eliminating crevice corrosion, was used for electrochemical polarization tests. The temperature controlled corrosion cell exposes a 1.0 in. diameter circular area of the surface for polarization measurements. A saturated calomel electrode (SCE) was used as the reference electrode, with a platinum wire loop as the counter electrode. Polarization curves were obtained at a scan rate of 1.2 V/hr from 0.1 V below the OCP until a current of 75 mA was achieved. All tests were performed at 25 C under constant aeration. A Brinkmann LB75L Laboratory Potentiostat was used with external computer control. The OCP was measured between the specimen and the SCE prior to initiating each polarization scan.

## RESULTS AND DISCUSSION

**Residual Stress Distributions.** The residual stress distributions measured as functions of depth and distance are shown graphically in Figures 2, 3 and 4. Compressive stresses are shown as negative values, tensile as positive, in units of ksi ( $10^3$  psi) and MPa ( $10^6$  N/m<sup>2</sup>). The residual stress results for the as-received (FSP only) condition are shown in Figures 2 and 3 for the directions parallel and perpendicular to the FSP tool path. Tension exceeding +200 MPA (+25 ksi) is present below the surface in the parallel direction at distances from 0 to nominally 1 in. from the last pass. These locations are on the last FSP pass. The perpendicular stresses are compressive or low magnitude tension.

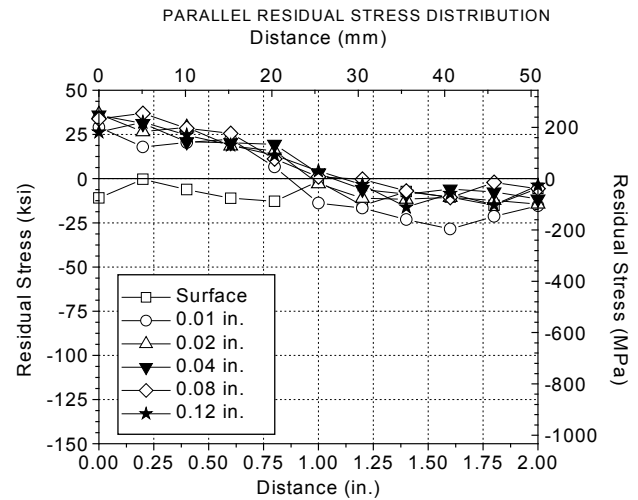


Fig. 2 – Parallel Residual Stresses in FSP Plate.

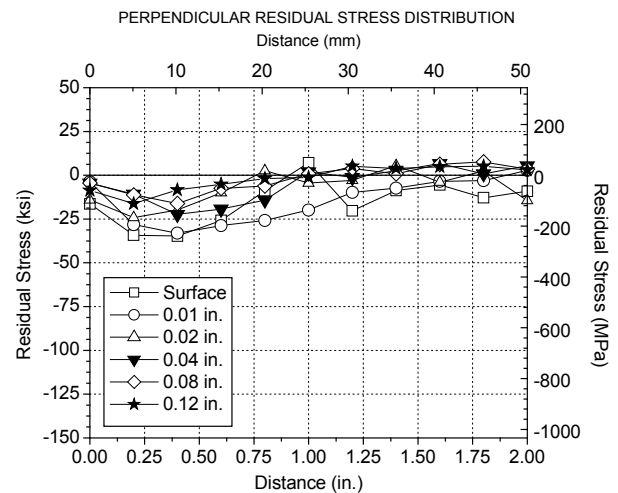


Fig. 3 – Perpendicular Residual Stresses in FSP Plate.

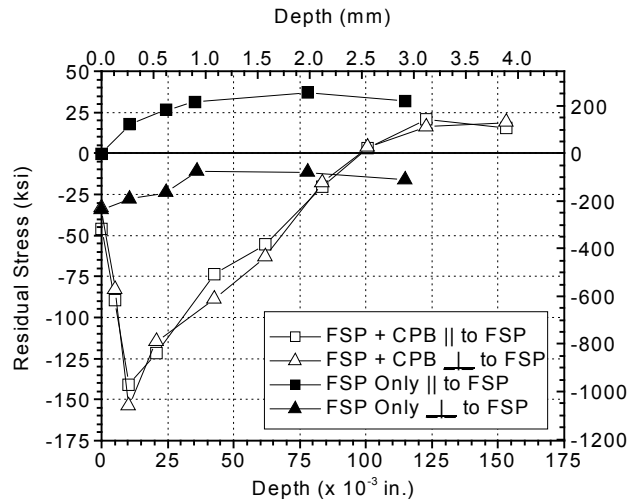


Fig. 4 – Residual stress as a function of depth in FSP + CPB and baseline (FSP Only) conditions.

The residual stresses from CPB are compared to the FSP results at the 0.2 in. location in Figure 4. CPB produces compression to a depth of 0.1 in. with magnitudes as high as -150 ksi.

### HIGH CYCLE FATIGUE TESTING.

The HCF results are presented graphically in Figure 5 as semi-logarithmic S-N curves fitted to a power law function. None of the material conditions exhibit endurance limit behavior or the existence of a true threshold fatigue stress. A bar chart of the fatigue strengths at  $10^7$  cycles is shown in Figure 6. As expected for the NAB alloy intended for marine service, the Baseline material has nominally the same fatigue strength (at  $10^7$  cycles) of 32 ksi regardless of salt-water exposure, which compares well with the published fatigue strength.[15] Only fatigue in the salt solution environment was considered for the remaining tests. The FSP material had substantially improved salt-water fatigue performance. CPB after FSP provides only a slight fatigue strength improvement over the FSP, confirming that FSP does not introduce a salt-water corrosion fatigue debit. The introduction of 0.040 in. deep FOD does drastically reduce the fatigue strength of FSP material, as expected for the introduction of a stress concentration factor. The FOD had a minimal effect on the fatigue performance of the FSP+CPB due to the depth of the compressive layer that exceeded the depth of the notch. CPB increased the  $10^7$  cycle fatigue strength by almost 3X, to 55 ksi, with a life increase of 100X, at, in specimens with a defect.

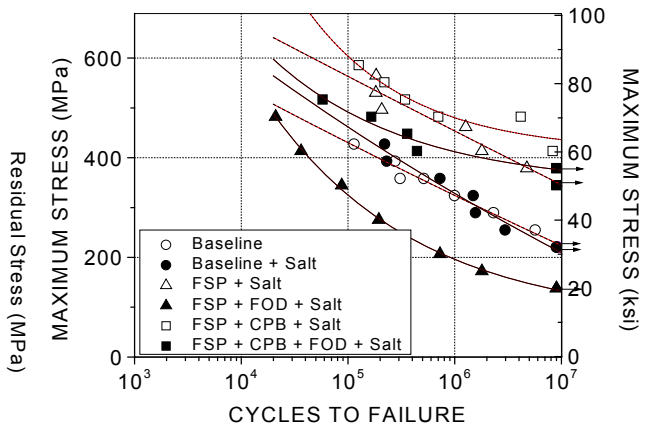


Fig. 5 - S-N Curve for NAB showing a nominal 3X increase in fatigue strength from CPB on specimens with 0.040 in. deep defect.

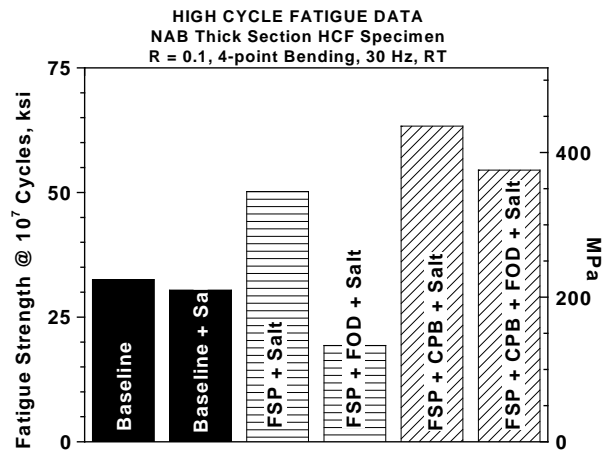


Fig. 6 – Fatigue Strength at  $10^7$  cycles.

Fractographic examination indicated that failure initiated at the surface of all samples without FOD except one FSP+CPB+salt specimen, which failed from below the surface due to the highly compressive surface layer. All specimens with FOD had failures that originated from the defect.

### ELECTROCHEMICAL POLARIZATION.

The OCP for the FSP and CPB surfaces is only very slightly increased over the OCP of the Baseline material in neutral salt solution. The average OCP values for three replicate tests of each finish are -0.265 V, -0.257 V, and -0.256 V for Baseline, FSP, FSP+CPB, respectively. FSP is 8 mV more positive than Baseline, and FSP+CPB is 9 mV more positive than Baseline. CPB and FSP are not significantly different in terms of the OCP.

The Baseline OCP shows a significant anodic shift in the acidic salt solution as compared to the neutral salt solution, while the FSP and FSP+CPB have minimal anodic shift. The average OCP values for three replicate tests of each finish are -0.350 V, -0.262 V, and -0.261 V for Baseline, FSP, and FSP+CPB, respectively. This indicates CPB+FSP and FSP have the most noble OCP's in the acidic salt solution, generally a benefit in terms of corrosion behavior.

Three replicate polarization curves were obtained with consistent results for each condition in both the neutral and acidic aerated salt solutions. The results in Figure 7 for the Baseline material compare very well to the results of Xue et al.[16] The OCP for the Baseline material is more negative (less noble) in the acidic solution than the FSP material. CPB has no effect on the OCP of the FSP material. There is no significant difference between the anodic polarization curves beyond the OCP for any material in either solution. The Baseline material shows a slightly larger increase in current towards the latter portion of each curve, however heavy pitting has already begun at this voltage for all specimens.

### CONCLUSIONS

Residual tension on the order of 30 ksi is present in the direction parallel to the FSP tool path in the region of the last FSP pass. The perpendicular stresses are compressive or low magnitude tension. CPB produces a depth of compression on the order of 0.1 in. with magnitudes as high as -150 ksi in the FSP material.

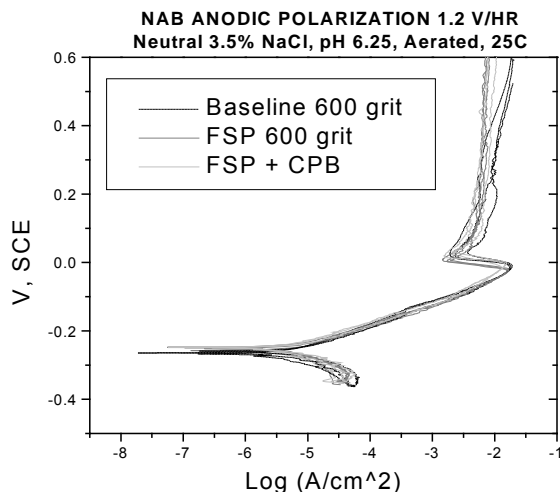


Fig. 7 - NAB Anodic Polarization in neutral 3.5% salt solution for Baseline, FSP, and FSP + CPB material

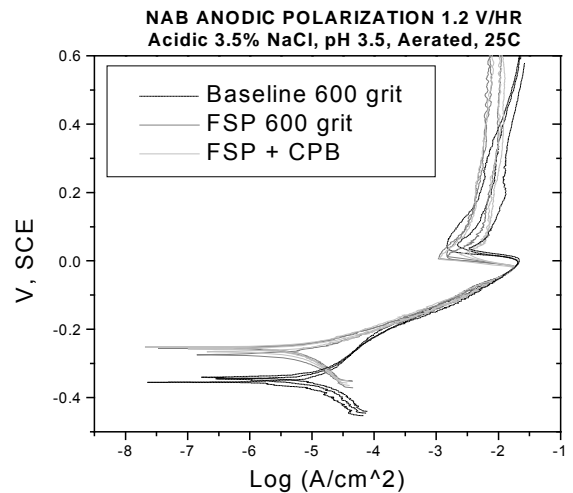


Fig. 8 - NAB Anodic Polarization in acidic 3.5% salt solution for Baseline, FSP, and FSP + CPB material. Note the higher OCP of the FSP and FSP + CPB material.

The fatigue strength of the Baseline cast NAB material was not reduced by exposure to neutral salt solution during fatigue cycling. FSP increases the fatigue strength of baseline cast NAB at  $10^7$  cycles from 32 ksi to nominally 55 ksi. The introduction of a 0.040 in. (1 mm) deep EDM defect reduces the strength of FSP to 20 ksi, or approximately one-third of its original strength. CPB increases the fatigue strength of FSP NAB by nominally 10% for specimens with no defect, and close to 300% for specimens with a 0.040 in. (1 mm) deep notch. The presence of the 0.040 in. defect imposed little to no degradation of fatigue strength on specimens that were CPB processed.

The OCP for FSP and FSP+CPB NAB is very slightly increased (more noble) than Baseline NAB in neutral salt solution. In an acidic salt solution the OCP of Baseline material decreased substantially (thus making it less noble), while the FSP and FSP+CPB materials showed little change.

On average, the FSP and FSP+CPB perform electrochemically the same in both neutral and acidic salt solutions throughout the range of polarizations studied. Beyond the OCP, the anodic polarization curves for NAB Baseline, FSP and FSP+CPB show no significant difference.

FSP of cast NAB material provides a 70% increase in fatigue strength over the cast material. CPB following FSP provides a further damage tolerance to notches up to 1 mm deep. Neither FSP or CPB render NAB susceptible to corrosion fatigue in neutral salt water, or degrade the corrosion resistance in either an acidic or neutral salt-water environment.

## REFERENCES

- [1] P. Prev y and M. Mahoney, "Improved Fatigue Performance of Friction Stir Welds with Low Plasticity Burnishing: Residual Stress Design & Fatigue Performance Assessment," Proc. Thermec, Madrid, Spain, July 7-11, 2003
- [2] P. Prev y, J. Telesman, T. Gabb and P. Kantzos, "FOD Resistance and Fatigue Crack Arrest in Low Plasticity Burnished IN718," Proc. 5th Nat.Turbine Eng. HCF Conference, 2000.
- [3] J. Cammett, P. Prev y, "Low Cost Corrosion Damage Mitigation and Improved Fatigue Performance of Low Plasticity Burnished 7075-T6," Proc. 4th International Corrosion Workshop, Aug. 22-25, 2000.
- [4] P. Prev y, M. Shepard and P. Smith, "The Effect of Low Plasticity Burnishing (LPB) on the HCF Performance and FOD Resistance of Ti-6Al-4V," Proc. HCF Conference, 2001
- [5] J. Cammett and P.S. Prev y, "Fatigue Strength Restoration in Corrosion Pitted 4340 Alloy Steel via Low Plasticity Burnishing" retrieved from [www.lambdatechs.com](http://www.lambdatechs.com), Feb. 2, 2006.
- [6] M. Hilley, ed., Residual Stress Measurement by X-Ray Diffraction, SAE HS-784, (Warrendale, PA: Society of Auto. Eng.), 1972.
- [7] I. Noyan, and J. Cohen, Residual Stress Measurement by Diffraction and Interpretation, (New York, NY: Springer-Verlag), 1987
- [8] B. Cullity, Elements of X-ray Diffraction, 2nd ed., (Reading, MA: Addison-Wesley), (1978) pp. 447-476.
- [9] P. Prev y, "X-Ray Diffraction Residual Stress Techniques," *Metals Handbook*, **10**, (Metals Park, OH: ASM), (1986), pp 380-392.
- [10] D. Koistinen, and R. Marburger, Transactions of the ASM, 67 (1964)
- [11] M. Moore, and W. Evans, "Mathematical Correction for Stress in Removed Layers in X-Ray Diffraction Residual Stress Analysis," SAE Transactions, **66**, (1958) pp. 340-345
- [12] P. Prev y, "A Method of Determining Elastic Properties of Alloys in Selected Crystallographic Directions for X-Ray Diffraction Residual Stress Measurement," Adv. In X-Ray Analysis, **20**, (New York, NY: Plenum Press, 1977), pp 345-354.
- [13] A. Al-Hashem, P. Caceres, W. Riad, and H. Shalaby, "Cavitation Corrosion Behavior of Cast Nickel-Aluminum Bronze in Seawater," Corrosion, Vol. 51, No. 5, (1995), pp. 334.
- [14] R. Qvarfort, "The Avesta Cell – A New Tool for Studying Pitting," Avesta Corrosion Management, No. 2-3, (1988), pp. 2-5
- [15] M. Prager, The Metal Properties Council, Inc., "The Properties of Cast Alloys for Large Marine Propellers," ASME Conference on Cast Metals for Structural and Pressure Containment Applications, (1979), pp. 238, American Society of Mechanical Engineers, New York, USA, BNF-63004
- [16] L. Xue, J.-Y. Chen, C. Hyatt, and M. Islam, "Laser Cladding with Continuous Ni-Al Bronze Wire Feeding for Repairing Marine Components," ICALCO, Vol. 87, Part 2, Section F, (1999), pp. 64.